Influence of asphaltene polarity on hydrate behaviors in water-in-oil emulsions

Dongxu Zhang[a], Qiyu Huang[a,*], Wei Wang[b], Rongbin Li[a], Huiyuan Li[c], Haimin Zheng[a], Xiangrui Zhu[a], Xun Zhang[a] and Yijie Wang[a]

[a]Beijing Key Laboratory of Urban Oil and Gas Distribution Technology/Surface Engineering Pilot Test Center, CNPC, China University of Petroleum, Beijing 102249, China

[b]SINOPEC Dalian Research Institute of Petroleum and Petrochemcials, Dalian 116000, China

[c]CNPC Research Institute of Safety Environmental Technology, Beijing 102206, China

ABSTRACT: Asphaltene was fractionated into four subfractions with different polarities, and used to conduct the hydrate formation and dissociation experiments. It was observed that the more polar fraction could result in a higher tendency of self-aggregation and fewer asphaltenes adsorbing at the water-oil interface mainly due to the larger C/H ratio, higher aromaticity, and shorter length of the alkyl side chain. The nucleation rate decreased with the presence of asphaltenes, and the induction time increased with a reduction in asphaltene polarity in water-in-oil emulsions. The results showed that the formed amount of hydrates were reduced by the addition of asphaltenes. For the asphaltene containing emulsions, less hydrate was formed with the presence of a more polar asphaltene fraction. The presence of asphaltenes was also found to affect the growth rate of hydrate, which varies with the polarity. Meanwhile, all four asphaltene fractions were found to promote the dissociation of hydrate.

Keywords: Hydrate formation; Water-in-oil emulsion; Asphaltene polarity; Interfacial adsorption; Flow assurance

1. Introduction

Gas hydrates are ice-like crystalline structures, and typically appear at low temperature under high pressure.[1,2] The deep offshore multiphase pipeline transporting oil, water, and natural gas provides a suitable condition for hydrate formation as the ideal pressure and temperature. Hydrates are considered as one of the major flow assurance threats, especially after the blockage occurred in natural gas transportation pipelines.[3,4] Hydrates plugging can cause huge economic and time loss once occurred. In order to avert the issue, two methods are usually adopted. One is thermodynamic hydrate inhibitors injection, aiming for the hydrate avoidance, including adding methanol or monoethylene glycol et al. The other one is the risk-management strategy through using the low dosage hydrate inhibitors, such as anti-agglomerants.[4] In under-water multiphase pipelines, the presence of waxes, asphaltenes, and resins in crude oils can influence the formation process of hydrate and consequently posing challenges to the management of hydrate. As a result, the hydrate formation and dissociation processes in water-oil pipelines with the presence of oil components, such as asphaltenes, need to be further investigated for the seeking of a deeper understanding.

Water is usually co-produced with oil.[5,6] The fluids in deep offshore multiphase pipelines are commonly in the form of water-in-oil emulsion due to the low water content and the existence of natural surfactants.[7] Thus, hydrate formation in water-in-oil emulsions has been increasingly investigated by researchers. Turner proposed a four-stage conceptual mechanism for explaining hydrate plugging in a multiphase flow system, including the steps of water entrainment, hydrate growth, agglomeration via capillary attraction, and catastrophic plugging.[8-10] In the past over decade, some researchers have paid attention to the issues of hydrate formation and tried to quantify the formation rate in water-in-oil emulsions. In 2009, Turner et al.[11] developed a mass transfer model to describe hydrate shell growth on the water droplet entrained in the oil phase, wherein gas diffused through the inward migrating shell into the water phase for hydrate growth. After that, an inward and outward shell model was presented to describe hydrate growth, considering the intrinsic kinetics, mass transfer, and heat transfer limitations by Shi et al.[12].

Dalmazzone et al.[13] hold that each droplet was an isolated micro-sized sample in the water-in-oil emulsion, and hence proposed the induction time model based on the normal distribution. In addition, the CSMHyK model was proposed and made a great contribution to a deeper understanding of hydrate growth, agglomeration, and plugging in the oil-dominated system.[14,15] Three sub-models of it were proposed by Turner and Boxall et al.,[8,14] i.e. the kinetics model, transport model, and cold flow model.

In actual under-water multiphase pipelines, crude oil is a complex mixture of waxes, asphaltenes, resins, and naphthenic acids, etc.[16] The behavior of hydrate formation is difficult to be completely understood and the formation models still cannot achieve good universality. Therefore, in recent years, researchers are increasingly paying attention to the effect of crude oil components on hydrate formation in water-in-oil emulsions.[7,17,18] As the heaviest and most polar component of crude oils, asphaltenes have interfacial activity.[19,20] They can adsorb at the water-oil interface and impede the coalescence of water droplets.[21] Asphaltenes in the crude oils may change the interfacial properties of water droplets and affect the behaviors of hydrates in the water-in-oil emulsion systems. Several works have been reported to investigate the effect of asphaltenes on hydrate formation in water-in-oil emulsions.[16,20,22] By the method of MD simulation, Zi et al.[20] found that asphaltenes can inhibit methane hydrate cage formation. They proposed that the two primary reasons for the phenomenon were the inhibition of gas solution by the asphaltene shell and the destruction of the hydrogen-bonded networks between water and gas molecules by asphaltenes.[20] Sandoval et al.[22] carried out CO_2 hydrate formation experiments using crude oils by adding various contents of asphaltenes, finding that asphaltenes cannot avoid hydrate formation but can increase the induction and growth time. They proposed that the mechanism of asphaltenes on hydrate formation was similar to kinetic hydrate inhibitors (KHI). For the formation process of the gas hydrates in the crude oils with different asphaltene contents, Daraboina et al.[16] observed that higher asphaltene and resin contents had a stronger inhibiting effect on hydrate formation. However, Stoporev et al.[23] didn't found a direct correlation between asphaltene content and hydrate formation rate.

Till date, the work on the effects of asphaltenes on hydrates in water-in-oil emulsions is still insufficient. To the best of our knowledge, crude oils or single "pseudo-component" asphaltenes are used in experiments to investigate the effects of asphaltenes on hydrate formation in the previous works. The influences of asphaltene polarity on gas hydrate nucleation, growth, and dissociation are still an open work. Asphaltenes with various polarities may present different interfacial activity, depending on their composition and structural characteristics. Fogler et al.[24,25] proposed the fractionation procedure for obtaining asphaltene subfractions with various polarities, and fractionated four asphaltene subfractions with different polarities through adjusting the volume ratio of a binary mixture of *n*-pentane and methylene chloride. They found that the structural characteristics including C/H ratio, specific surface area, and stability of asphaltene were demonstrated to be strongly related to the polarity. The asphaltene polarity has been considered a research hotspot after that in the field of crude oil, especially in the study of wax precipitation and deposition.[26-29] The particle diameters and aggregation behavior of asphaltenes can be also influenced by the polarity of asphaltenes.[26] Moreover, the different polarity asphaltenes with various structural characteristics and existence states may influence the adsorption process of asphaltenes and the interfacial properties of water droplets, which can lead to different behaviors of hydrates in water-in-oil emulsions. The fundamental understanding of the influence of asphaltene polarity on gas hydrate formation and dissociation processes, which is currently lacking, will provide deeper insights into the interactions between hydrates and asphaltenes in the flow assurance issues. The practical, as well as academic interest, encouraged us to do this work.

In this study, the influences of asphaltene polarity on hydrate nucleation, growth, and dissociation processes were investigated for preliminary understanding. Four subfractions of the asphaltene with different polarities were fractionated and employed for the purpose. Synthetic model oils were used for the control of asphaltene polarity and concentration, wherein the asphaltene in the mode oil was maintained at 0.15 wt %.[30,31]

2. Experimental section

2.1 Materials

In the present work, asphaltenes were separated from a Venezuela residue oil, following the standard procedure of ASTM D6560-2017. The four subfractions were fractionated using an adjusted fractionation procedure developed earlier in Folgler's group.[24,25] The fractionation procedure is outlined in Figure 1. The asphaltene was first dissolved in dichloromethane at 1:10 (w/w). Binary mixtures of *n*-pentane and dichloromethane solvents with various volume ratios were used for fractionation. Pentane was added to the dichloromethane-asphaltene mixture until the solvent ratio of dichloromethane and pentane at 33:67 (v/v), and then the fraction $F_{33/67}$ was obtained by centrifuging for 30 min at 500 rpm. In a similar manner, the second, third, and fourth subfraction, i.e. $F_{25/75}$, $F_{20/80}$, and $F_{10/90}$ were achieved. As shown in the procedure, the most polar fraction is $F_{33/67}$.[24] The key elemental and structural parameters of the four fractions are shown in Table 1, more details of the characterization of the four asphaltene fractions can be found in the previous work.[29] CO_2 was supplied by HTJK Gas Technology Company, Limited (Beijing, China), 99.99% purity. The 10# mineral oil obtained from Hasitai Oil Company, Limited (Shanghai, China), cyclic n-alkanes dominate. DI-ionized water through the experimentation collected from a water purification machine. *O*-xylene provided by Aladdin Group Company, Limited (Shanghai, China).

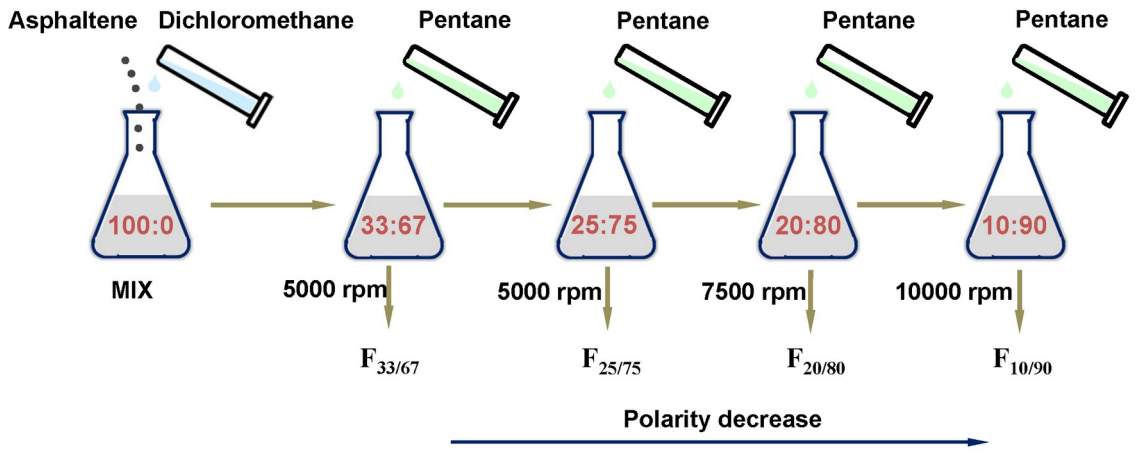

Figure 1. Fractionation procedure for different polarity subfractions, here, the ratios represent the dichloromethane: pentane in the mixture.

Table 1. Elemental and structural parameters of the four subfractions.[29]

	Definition	$F_{33/67}$	$F_{25/75}$	$F_{20/80}$	$F_{10/90}$
C (wt %)	carbon concentration	83.33	83.22	83.19	83.13
C/H	ratio of carbon to hydrogen concentration	0.91	0.90	0.89	0.86
n	number of structure units per molecule	7.77	6.57	5.67	5.99
L	relative length of alkyl side chain	3.42	3.84	4.30	4.16
f_a	fraction of aromatic carbons (aromaticity)	0.52	0.51	0.50	0.48

2.2 Experimental apparatus

The hydrate investigation apparatus is a self-designed high-pressure autoclave, which can be seen in Figure 2. A 16 cm inner diameter and 4.5 L effective volume chamber is the main reaction part. A feature of the apparatus included an on-line viscometer.[32] This allowed for measurement of system viscosity and determination of hydrate growth onset. Temperature of the system was controlled by the water bathes. The temperature, pressure, gas flow rate, and shear rate were monitored by a PT100 platinum resistance thermometer, a pressure transducer, a gas flow meter, and a tachometer, respectively. At the same time, the parameters were acquired and recorded by a computer. The apparatus and operation principles of the on-line viscometer were described in detail elsewhere.[32,33]

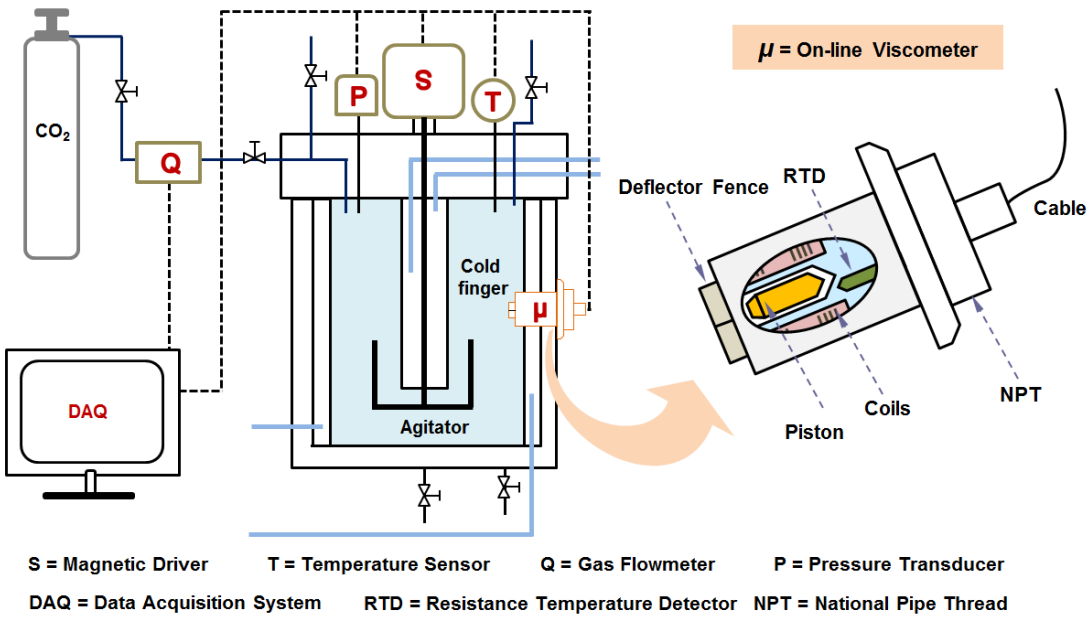

Figure 2. Schematic of the high pressure autoclave used herein.

2.3 Model oil and emulsion preparation

Asphaltene was required to be dispersed into the oil to obtain model oil. According to previous works of Li et al.[29], asphaltene was first completely dispersed in *o*-xylene by ultrasonic treatment at 65 °C for 15 min, and then mixed with the mineral oil using the IKARW 20 Digital to get the model oil. Then the de-ionized water was added to the model oil and the emulsion was prepared through stirring at 800 rpm for 30 min.[33] The ratio of water and model oil was kept at 20:80 (v/v) through the experimentation.[32] Moreover, droplet size distribution was measured to reflect the stability of the asphaltene containing emulsions. A Nikon OPTIPHOT2-POL polarizing microscope equipped with a Linkam PE60 cooling station was used for the purpose.

2.4 Hydrate formation procedure

Before the experiments, petroleum ether and de-ionized water were poured into the autoclave in turn to clean the chamber and viscometer, and the cleaning process was repeated twice.[7] The emulsion was poured into the thoroughly cleaned autoclave, then the chamber was covered and sealed, and the viscometer was connected. Prior to the pressuring process, the decompression valve was opened and CO_2 was injected into the autoclave for 15 min to remove the residual air.[32] Afterwards, the decompression valve was closed, and CO_2 was continuously added into the autoclave until the target pressure was reached. The emulsion was cooled to the target value after the pressurization, and then maintained at the temperature until the end of the hydrate formation experiment. During the cooling stage, the gas flow was constantly adjusted by controlling the pressure regulating valve, therefore, the pressure of the autoclave was maintained at the target temperature. The stirring rate was maintained at 300 rpm in all experiments.[33] Herein, the time zero of the hydrate formation experiment was defined as the pressuring onset.

2.5 Hydrate dissociation procedure

The dissociation process was adjusted based on the procedure used in Song's work.[34] The stirring rate was kept at 300 rpm and the pressure of the autoclave was reduced to 0.01 MPa higher than

the equilibrium value. Following this, the temperature of the water bath was increased by 20 °C at a constant heating rate.[34] The temperature of the water bath was then maintained at 20 °C for 30 min in order to fully dissociate the hydrates.

Two different series of experiments were conducted to investigate the effect of asphaltene polarity on hydrate behaviors in the asphaltene containing emulsions. The specific experimental condition and composition are listed in Table 2. The typical experimental temperature and pressure were selected according to the actual operation condition of underwater multiphase pipelines.[3,35,36] Besides, the parameter data versus time of three runs for the hydrate formation process in the emulsion with fraction $F_{10/90}$ are shown in Figure 3, illustrating the good repeatability of the measured parameters and calculated gas consumption for the hydrate formation process.

Table 2. Experimental condition and composition of emulsions in the work.

Exp.	Experimental condition			Composition of emulsions			
	Target pressure (MPa)	Target temperature (°C)	Cooling rate of water bath	Water volume (mL)	Asphaltene content (wt %)	O-xylene content (wt %)	Asphaltene polarity
Series 1	3	3.4	1 °C/10min	300	0.15	5	Control[a], o-xylene[b], $F_{33/67}$, $F_{25/75}$, $F_{20/80}$, $F_{10/90}$
Series 2	2.8	2.1	1 °C/15min	200	0.15	5	Control, $F_{33/67}$, $F_{25/75}$, $F_{20/80}$, $F_{10/90}$

[a]control refers to the system in the absence of asphaltene and *o*-xylene.

[b]*o*-xylene refers to the system just with *o*-xylene.

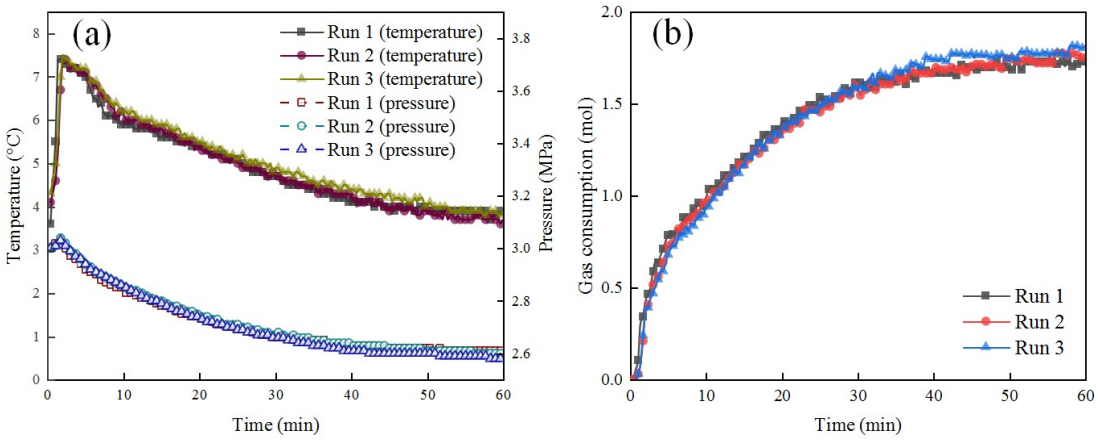

Figure 3. (a) Temperature, pressure and (b)gas consumption data versus time of the three hydrate formation runs for the emulsion with fraction $F_{10/90}$.

3. Results and discussions

Typical trends for the temperature, pressure, and viscosity during the hydrate formation and dissociation processes are shown in Figure 4. For the hydrate formation process, as shown in Figure 4a, three regions can be observed:

Region I was the pressurization stage. CO_2 was dissolved into the liquid and the system was continuously pressurized. The viscosity of the emulsion decreased due to the gas dissolution.

Region II was the cooling stage. The system was gradually cooled to the target temperature and maintained at a constant until the end of hydrate formation. According to previous studies,[37-39] the induction time of hydrate was determined form the time point when the system entered the phase equilibrium region and to the time point when the temperature increase suddenly.

Region III began as the temperature and viscosity increased suddenly, which signaled the completion of hydrate nucleation and the onset of hydrate growth. The pressure curve gradually decreased as gas consumption.

Figure 4b shows the temperature and pressure profiles during the process of hydrate dissociation. The increasing rate of temperature for the system was significantly lower than that of water baths in the first 35 min. This phenomenon was mainly caused by hydrate dissociation

as it was an endothermic process. During this process, a dramatic increase in pressure was found due to gas release by hydrate dissociation. As hydrates gradually dissociated and disappeared, the temperature increased rapidly due to less heat was adsorbed for hydrate dissociation, wherein the increase rate of the system was consistent with that of the water bath.

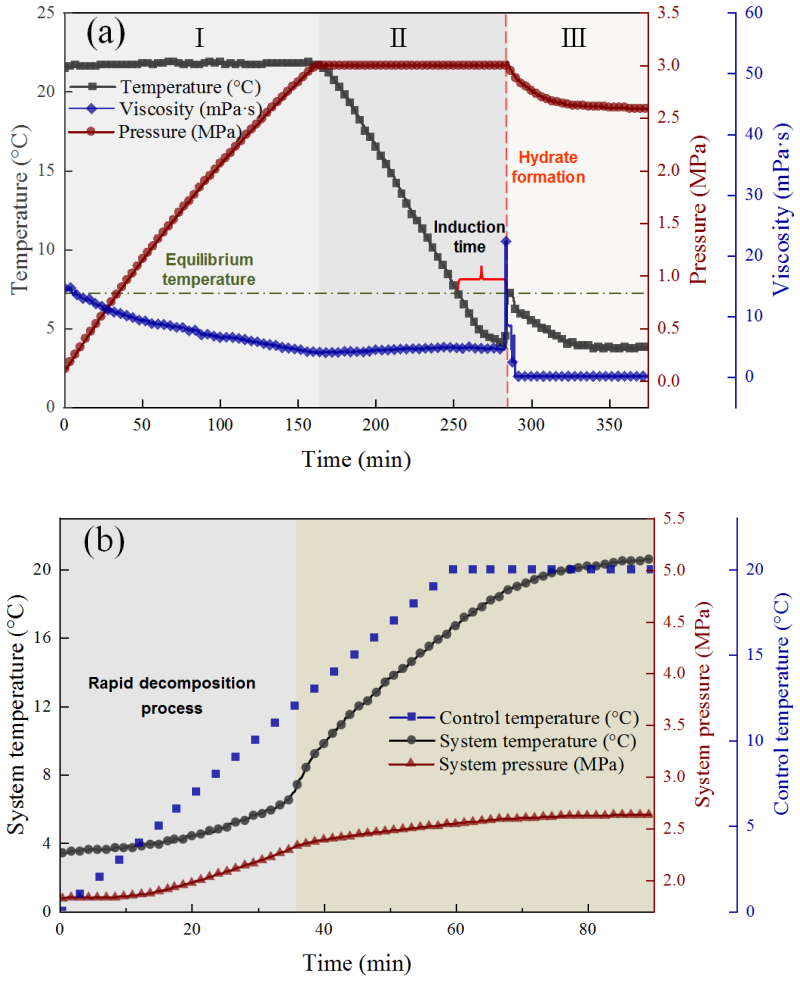

Figure 4. (a) Temperature, pressure, and viscosity trends during the hydrate formation process, and (b) temperature and pressure profiles in the hydrate dissociation process in the system with the presence of fraction $F_{20/80}$. Herein, control temperature refers to adjust the temperature of the water bath.

3.1 Morphology and micrograph of the four asphaltene fractions

The physical appearance of the four asphaltene fractions is shown in Figure 5. The particles of fraction $F_{33/67}$ were shiny and hard, while fraction $F_{10/90}$ consisted of dull and soft particles. The

physical appearance was in accordance with the observations of Nalwaya et al.[24], indicating the crystallinity and its order in the more polar asphaltene fraction increased.

The micrographs of asphaltenes in the model oils are obtained by the polarizing microscope, taking in the magnification of 10×20, and shown in Figure 6. It was observed that the more polar asphaltene fraction has a stronger tendency to self-aggregate. The diameter of asphaltene particles decreased with a reduction in polarity, which was in accordance with the observations of Liu et al.[40]. This phenomenon may be determined by the structural and compositional characteristics. The low C/H ratio and f_a can favor the dispersion of asphaltene particles.[29,41] Moreover, the oil compatibility of asphaltenes can be promoted by the large amounts of aliphatic groups and low condensed aromatic cores.[26] The less polar asphaltene fraction has a longer relative length of alkyl side chain, smaller number of structure units per molecule, and lower C/H ratio and f_a, which can be seen in Table 1. Therefore, the less polar asphaltene fraction has a higher tendency of dispersion in the model oils as the consequence of these structural and compositional characteristics. The fractal box dimension was widely used to clarify the complexity of wax crystals in oils, i.e. the higher fractal box dimension value represented the higher complexity of wax crystal morphology.[29,42] Applying the same approach, the fractal box dimension of asphaltenes was processed by Image J software,[42] based on the micrographs. As shown in Figure 7, the fractal box dimension of asphaltenes reduces from 1.53 (±0.14) to 1.30 (±0.01) with the reduction in polarity, corresponding to a decline up to 15%. This result indicated that the more polar fraction of asphaltenes were more complicated in the model oil, which can be attributed to the larger aggregates caused by stronger interaction of asphaltenes with more condensed aromatic cores and higher f_a.[29]

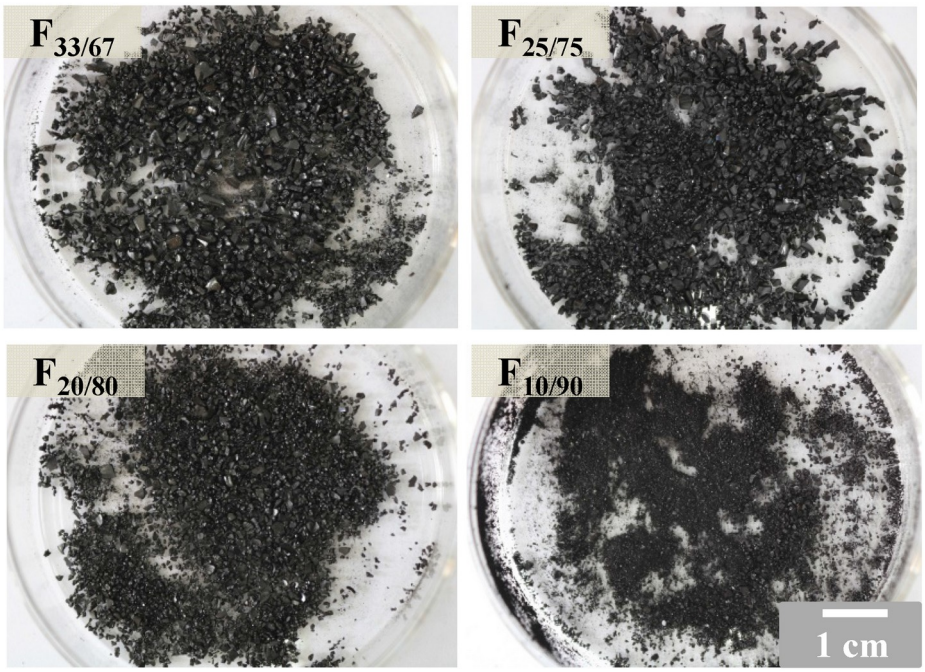

Figure 5. Physical apperance of the asphaltene fractions with different polarities.

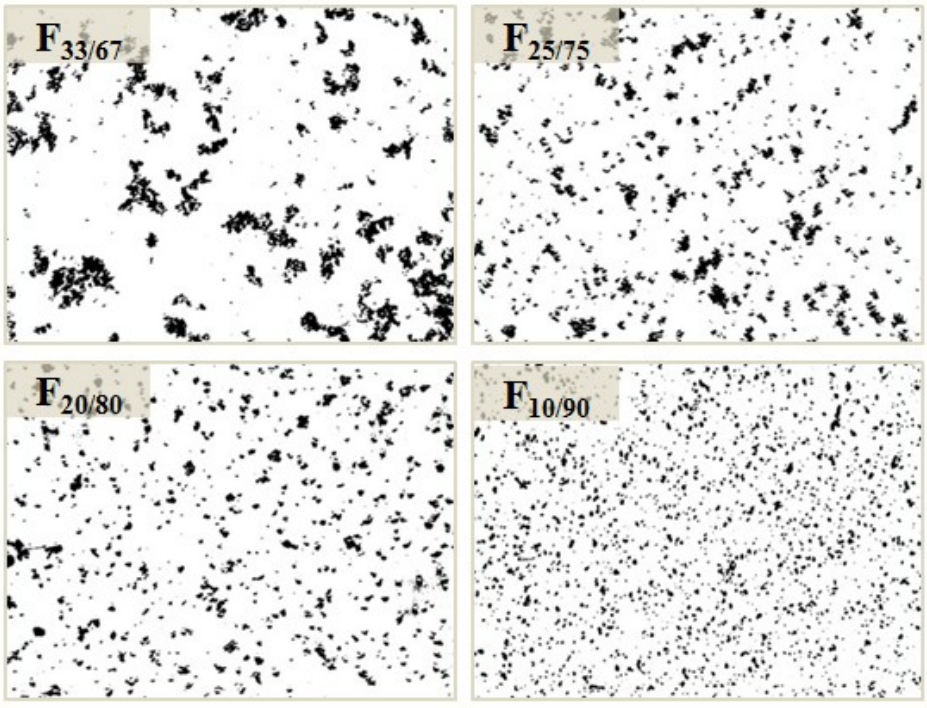

Figure 6. Microscope photographs of the asphaltene fractions in the model oil.

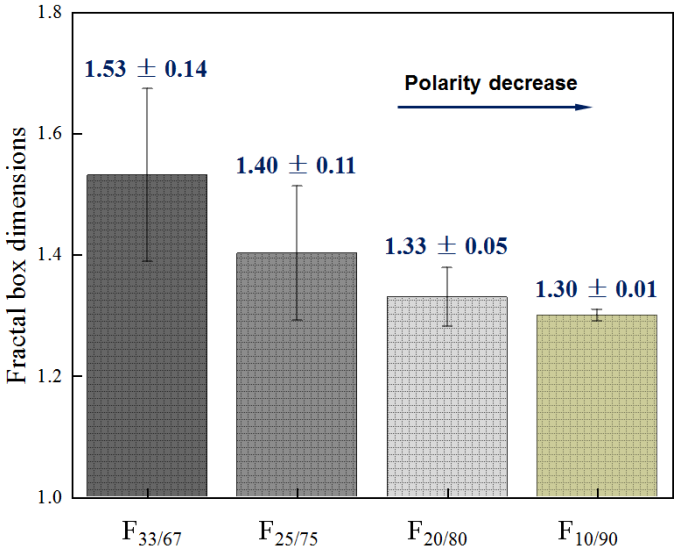

Figure 7. Fractal box dimensions of the four asphaltene fractions in model oil.

The morphologies of the emulsions with the presence of different polarity asphaltene fractions are displayed in Figure 8. The emulsion with the presence of fraction $F_{33/67}$ was black, and it becomes lighter with the reduction in polarity, till to brown of the emulsion with fraction $F_{10/90}$. The difference in the morphology may be attributed to the C/H ratio and the aromaticity. Specifically, the higher carbon concentration and more aromatic groups of more polar asphaltene fraction may lead to a darker appearance. Moreover, the water droplet size distributions of the four emulsions were determined by the microscope and Nano Measure 1.2 software.[43] The gray line in Figure 9 shows the droplet size distribution after emulsified. According to the experimental results in this work, the maximum time interval from emulsion preparation to hydrate formation was less than 7 h. Considering this, the droplet diameter distributions of the four systems after settling 7 h (circular symbols in Figure 9) were obtained to characterize the stability of the emulsion. Meanwhile, the diameter data were also measured under the continuous stirring station at 300 rpm after emulsified (triangle symbol in Figure 9), in order to more accurately reflect the parameters of droplet size in the dynamic stirring process during hydrate formation. As shown in Figure 9, the water droplets of the emulsion with the presence of the more polar asphaltenes are generally larger in size compared to that in the emulsion with the less

polar asphaltene fraction. Specifically, the diameters were 13.4, 12.2, 10.4, and 8.7 μm after emulsification in the emulsion with fraction $F_{33/67}$, $F_{25/75}$, $F_{20/80}$, and $F_{10/90,}$ respectively. Moreover, the emulsion with the presence of less polar fraction presented greater stability. As a natural surfactant, asphaltenes can be adsorbed at the water-oil interface, stabilizing the emulsion and inhibiting water droplet coalescence.[19,44] The adsorbed amount of asphaltenes can be decreased by the formation of aggregates.[21] For the emulsion with the more polar asphaltene fraction, the larger asphaltene particles caused by the higher tendency of self-aggregation can decrease the specific surface area of asphaltene, leading to fewer amounts of asphaltenes adsorbed at the water-oil interface. Therefore, the greater stability was observed in the emulsion with less polar fraction and the mean water droplet diameter in the emulsions decreased with a reduction in asphaltene polarity.

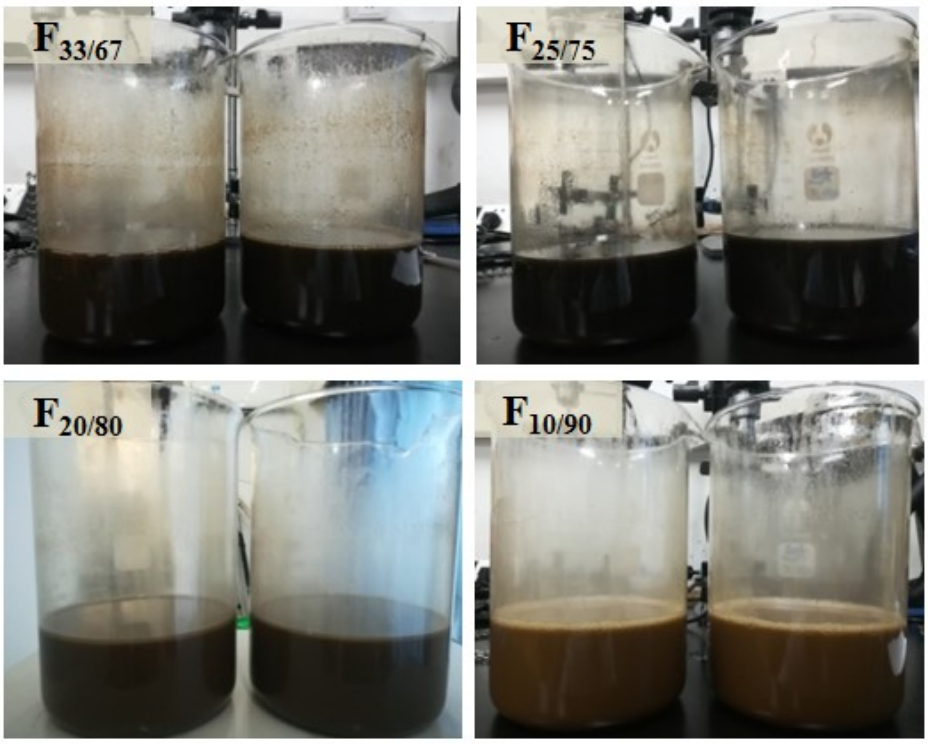

Figure 8. Morphologies of the emulsions with 0.15 wt % asphaltene content of different polarities.

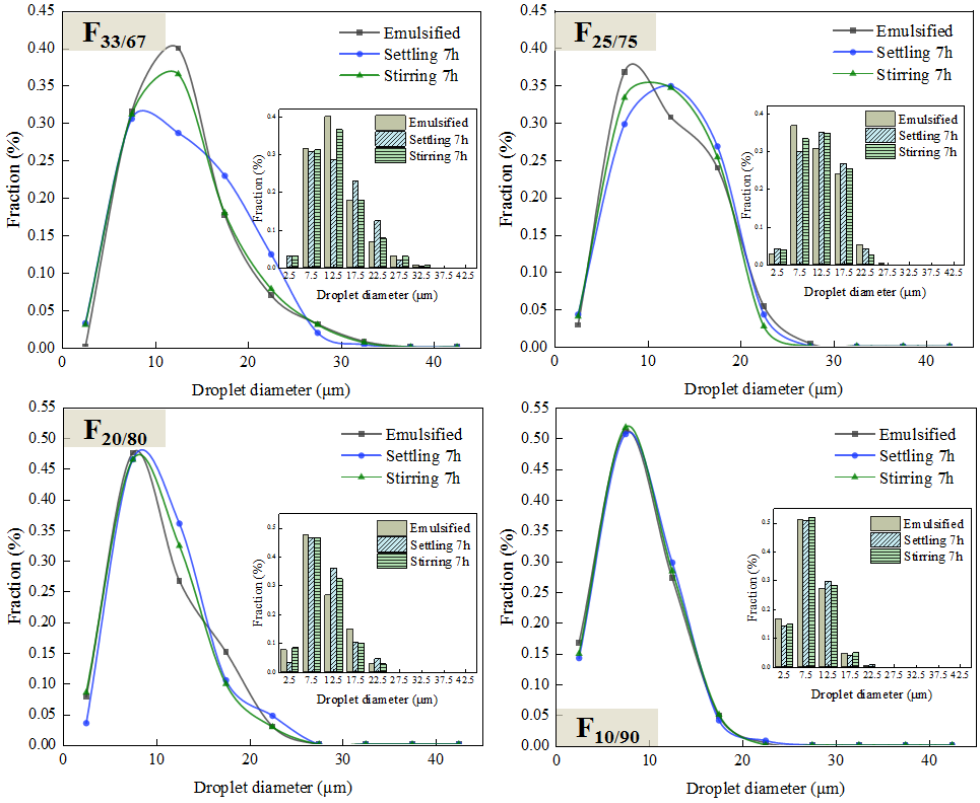

Figure 9. Size distribution of water droplets in the emulsions at the temperature of 3.4 °C.

3.2 Influence of asphaltene polarity on hydrate nucleation

Figure 10 shows the induction times of the various systems. It can be found that the induction time of hydrate in the emulsions with various asphaltene subfractions were all longer than that without asphaltenes. The induction time of the emulsion only with *o*-xylene is almost the same as that of the system with the absence of *o*-xylene and asphaltene, suggesting that the *o*-xylene has no obvious influence on hydrate nucleation. It was found that the induction time increased with the decreasing of asphaltene polarity, indicating that the less polar asphaltene had a stronger inhibiting effect on hydrate nucleation. In Series 1 experiments, for example, the induction time of hydrate in the emulsion with the absence of asphaltene was generally 22.0 min, while it was 43.3 min in the emulsion with the fraction $F_{10/90}$.

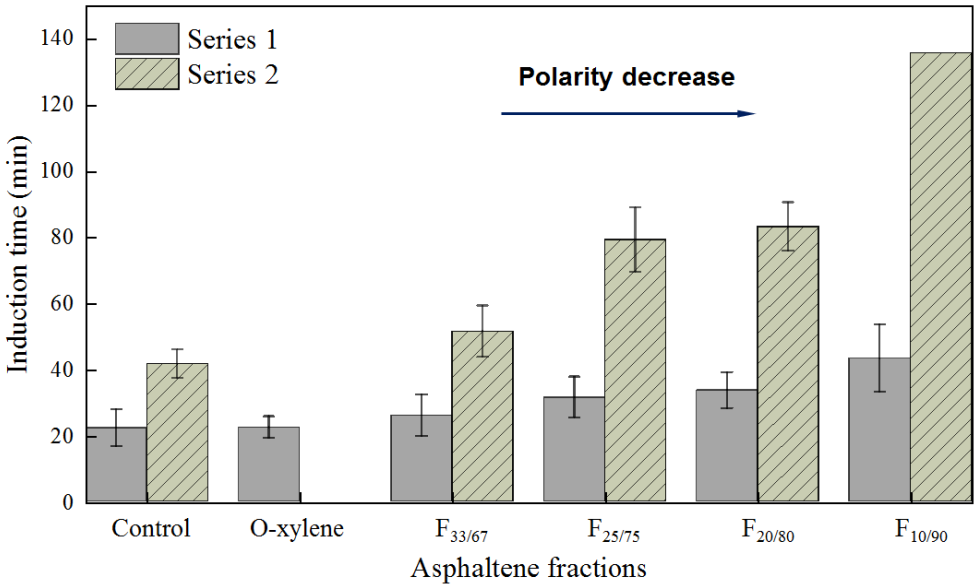

Figure 10. Influence of asphaltene polarity on hydrate induction time.

To have a deeper understanding of the asphaltene polarity on hydrate nucleation, the asphaltene presence state in the water-in-oil emulsion was observed by the polarizing microscope. As shown in Figure 11, large asphaltene aggregates are observed in the bulk with fraction $F_{33/67,}$ which is circled by the dotted line. The size of the aggregate greatly reduced in the emulsion with $F_{25/75}$ and $F_{20/80}$ compared with that in the emulsion with fraction $F_{33/67}$. This was because the more polar asphaltene fraction has a higher tendency of self-aggregation, as discussed in the above section. For the emulsion with the least polar asphaltene fraction (fraction $F_{10/90}$), no obvious asphaltenes can be found, but the rigid film and contracted interface was more apparent. Similar results of the rigid film can be found in the studies conducted by Czarnecki et al.[45] and Dabros et al.[46], which demonstrated that the water-oil interface transited from flexible to rigid caused by the adsorption of asphaltenes. These observations indicated that the less polar asphaltene fraction has higher adsorption efficiency at the water-oil interface. The adsorbed asphaltenes contributed to droplet coalescence inhibition and emulsion stability.[47] Therefore, the mean water droplet size was observed to decrease in the emulsion with the decreasing of the asphaltene polarity, as shown in Figure 9 in the above section.

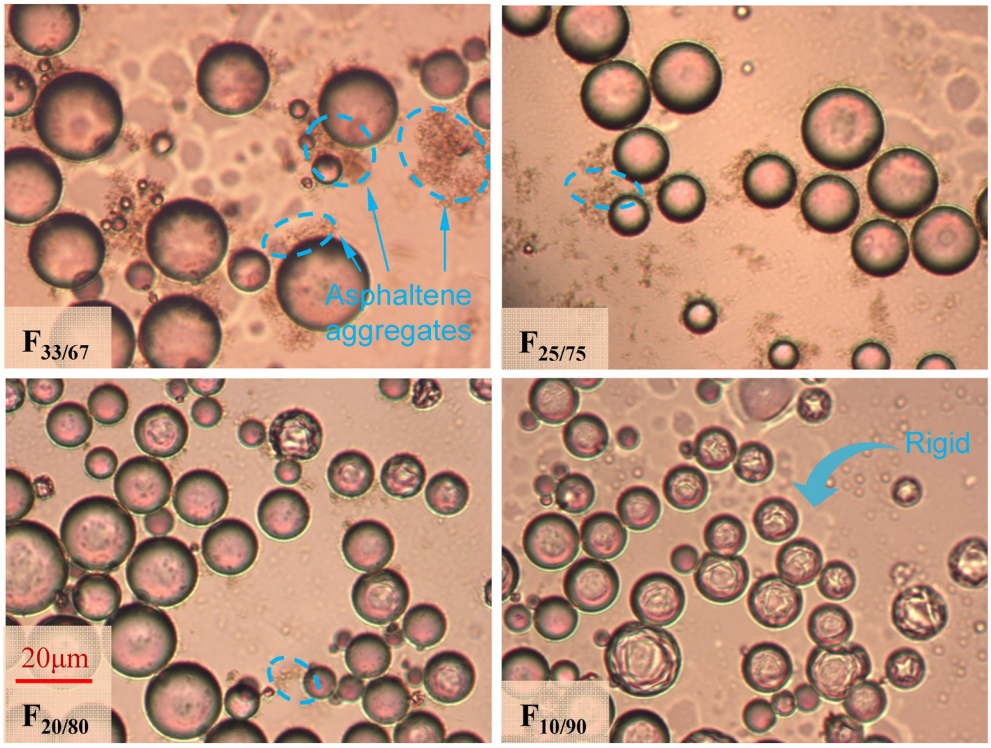

Figure 11. Microscope photographs of the emulsions with different polarity asphaltenes.

Hydrates nucleated at the water-oil interface in water-in-oil emulsions.[33] During the nucleation process, labile molecular clusters formed at the interface, consuming the gas molecules. The critical dimension crystal nucleus formed by the aggregation of molecular clusters appeared when the energy barrier was overcome, after which the crystal nucleus entered a period of rapid growth.[48,49] The adsorbed asphaltenes can decrease the available water-oil interface for hydrate nucleation, and restrict the diffusion of CO_2 to the water phase and the hydrate nuclei. In addition, the interaction between the water and guest molecules would be interrupted by the adsorbed asphaltenes.[20,22] Therefore, the nucleation rate was decreased in the emulsion with the presence of asphaltenes. Moreover, the inhibition effect on hydrate nucleation was more pronounced in the emulsion with the less polar asphaltene fraction. Thus, the induction time increased with a reduction in asphaltene polarity in the water-in-oil emulsions.

3.3 Influence of asphaltene polarity on hydrate growth

To obtain insights into the hydrate growth process with the presence of different polarity asphaltenes, the temperature and pressure profiles were captured and depicted in Figure 12 and 13. The gas mole consumption was calculated to quantitatively characterize the growth rate of hydrates by[32,50]

$$n = n_{\text{total}} - \frac{P_t V}{Z_t R T_t} - n_t \quad (1)$$

$$Z_t = f(T_t, P_t) \quad (2)$$

$$n_t = f(T_t, P_t) \quad (3)$$

where n_{total} is the total mole number of the gas in the autoclave before hydrate nucleation, which can be calculated based the gas flowmeter; P_t and T_t represent the pressure and temperature at time t; Z_t is the compressibility factor, calculated by the Soave-Redlich-Kwong equation of state;[51] n_t is the mole number of the gas dissolved in the emulsion at the condition of P_t and T_t.

As shown in Figure 12a-e and 13a-e, temperature increases rapidly to the peak within 5 min due to the highly exothermic growth of hydrate. The growth rate would be decreased as the hydrate shell gradually thickens.[11,12] and hence, the released heat decreased accordingly. On the other hand, the circulating coolant bath could continuously take away the released heat through heat exchange. Thus, the temperature of the system then decreased when the released heat was less than that taken away. The peak of the system with Fraction $F_{25/75}$, $F_{20/80}$, or $F_{10/90}$ was 7.5 °C, which is higher than the system without asphlatenes (7.1 °C), in Series 1 experiments. However, the system with fraction $F_{33/67}$ is lower (5.2 °C, as shown in Figure 12e). Figure 12f and 13f show gas consumption during hydrate growth for the various systems. It can be found that the fraction $F_{25/75}$, $F_{20/80,}$ and $F_{10/90}$ can promote gas consumption, while the fraction $F_{33/67}$ hindered it. In addition, the initial gas consumption rate for the initial hydrate growth stage (herein, it was determined from the growth onset to the temperature peak, see the gray region) in the asphaltene containing systems was calculated by

$$R_{\text{initial}} = \frac{n_{\text{initial}}}{t_{\text{peak}} - t_{\text{onset}}} \tag{4}$$

where $n_{initial}$ is the cumulative mole number of gas consumption during the initial hydrate growth stage; t_{peak} and t_{onset} are the time when the temperature reaches its peak and the growth onset. Figure 14 shows the data of the initial gas consumption rate for different conditions. These results suggest that the fraction $F_{33/67}$ decreased the hydrate growth rate, but the other three less polar asphaltene fractions increased it in the initial hydrate growth stage.

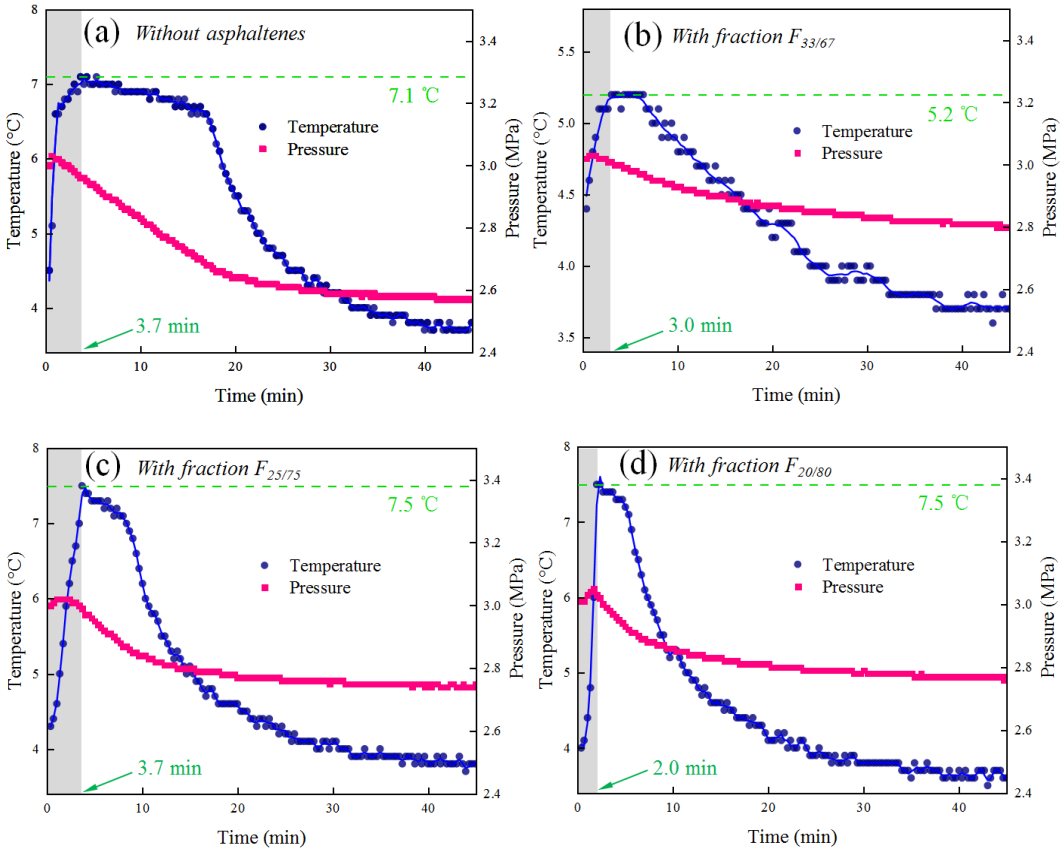

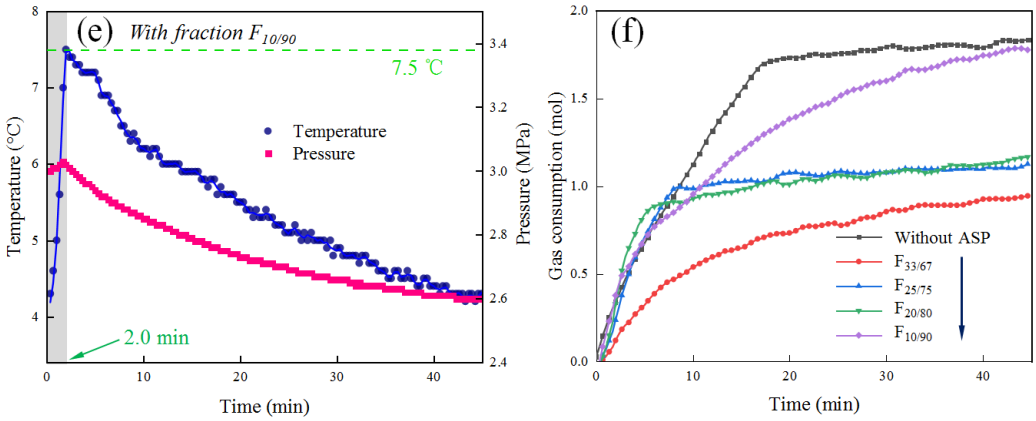

Figure 12. Temperature and pressure profiles of Series 1 experiments during hydrate growth stage for the system (a) without asphaltenes and with the presence of fraction (b) $F_{33/67}$, (c) $F_{25/75}$, (d) $F_{20/80}$, and (e) $F_{10/90}$. (f) Cumulative gas consumption curves during hydrate growth in the presence of various polarity asphaltene fractions.

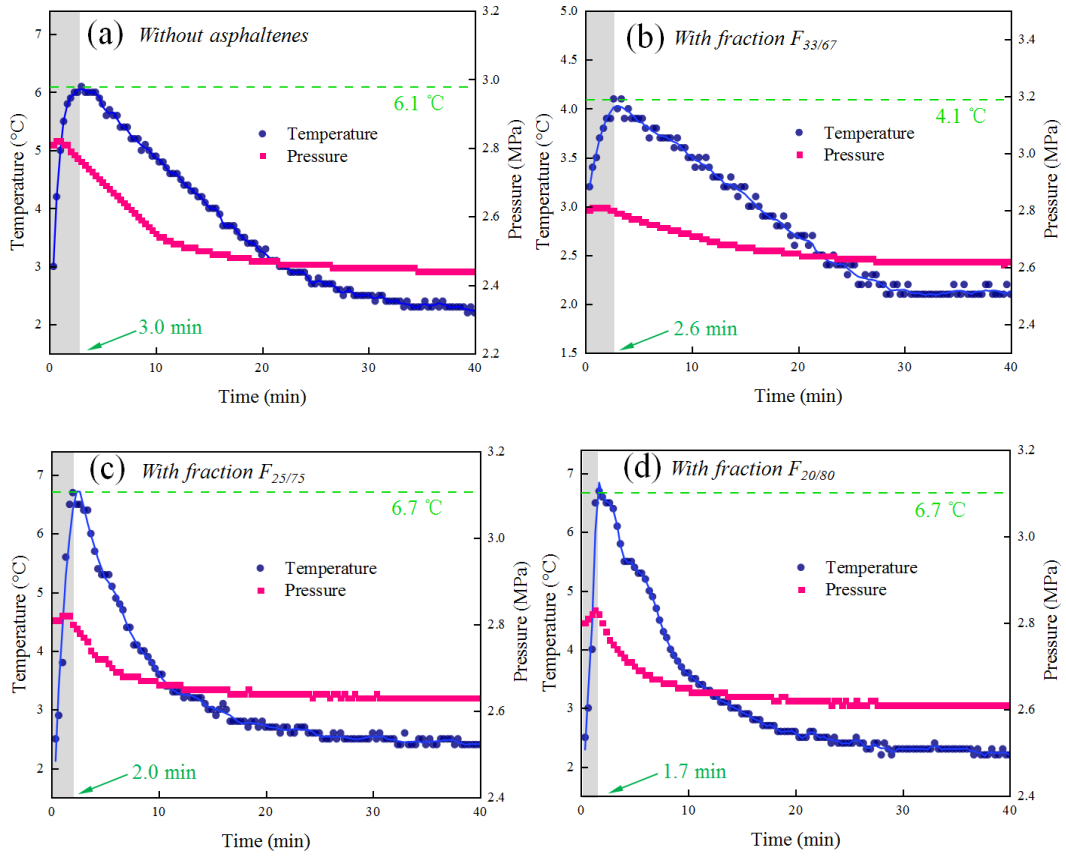

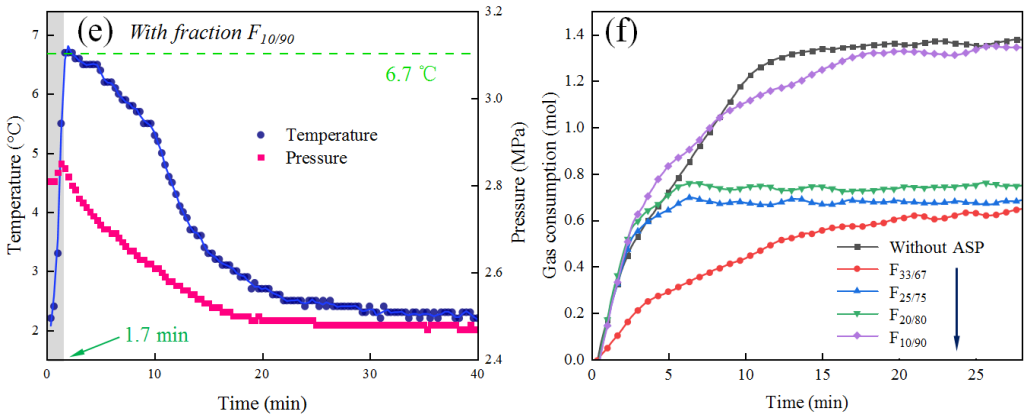

Figure 13. Temperature and pressure profiles of Series 2 experiments during hydrate growth stage for the different systems (a-e). Cumulative gas consumption curves during hydrate growth (f).

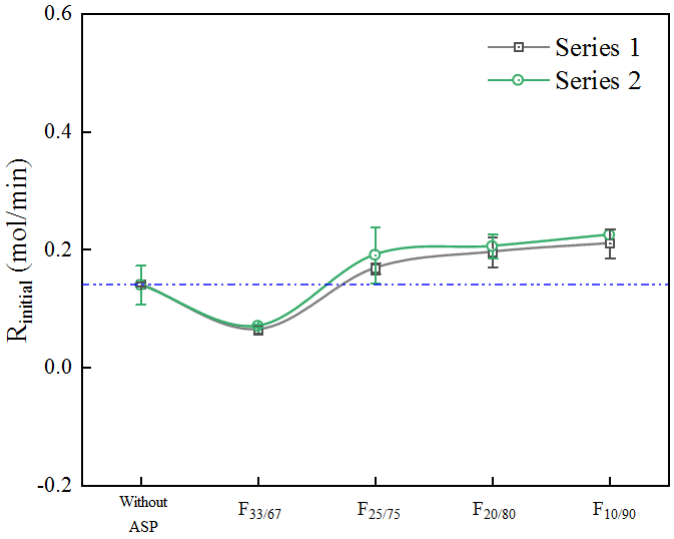

Figure 14. Initial gas consumption rate during hydrate growth in the systems with various polarity asphaltenes.

The growth of hydrate in water-in-oil emulsions was determined by heat and mass transfer, droplet surface area, and intrinsic kinetics.[11,52] During the process of hydrate growth, the dissolved gas was rapidly consumed for hydrate shell formation, decreasing the gas concentration near the water-oil interface.[53] Therefore, the concentration gradient of gas caused the rapid mass transfer of dissolved carbon dioxide to diffuse from the bulk to the water phase.

The different effects of various polarity asphaltenes on hydrate growth rate could be attributed to two factors: (1) water droplet size, and (2) gas molecules trapped in asphaltene aggregates.

The smaller water droplet provided the larger water surface area for hydrate shell formation and growth. Therefore, for the system with fraction $F_{25/75}$, $F_{20/80,}$ or $F_{10/90}$, more heat was released due to the larger surface area of water conversion in the initial growth stage. For the system with fraction $F_{33/67}$, however, the temperature peak and gas consumption were both decreased, though the water droplet diameter can be also lowered comparing to the system without asphaltenes. This result could be attributed to the trapping of gas molecules in the large asphaltene aggregates. According to the results of MD simulation and experiments conducted by Li et al.[54] and Dmitrievskii et al.[55], CO_2 molecules would be adsorbed on the asphaltene aggregates due to the large free volume fraction, surface area, and intermolecular interaction. Therefore, the growth rate was decreased due to the reduction in gas supply for hydrate formation in the system with the presence of fraction $F_{33/67}$. In addition, some researchers found that the adsorbed KHI can increase the hydrate growth rate by increasing the hydrate shell porosity, even though it inhibited hydrate nucleation.[56-58] On account of this, the hydrate shell porosity change could be a potential influencing factor for hydrate growth in the systems with asphaltene fraction $F_{25/75}$, $F_{20/80,}$ and $F_{10/90}$, which should be investigated by microscopic instruments in the future.

The hydrate formation experiments ended when hydrate was formed for 90 min. Figure 15a shows the total gas consumption due to hydrate formation. The amount of formed hydrates in the system without asphaltenes is higher than that in the system with the presence of asphaltene fractions. According to Turner et al.[35], during the hydrate formation process in water-in-oil emulsions, the water droplet can be seed and direct converted by collision with a hydrate particle, as shown in Figure 15b. However, the adsorbed asphaltenes around the water droplet can inhibit the direct conversion in the emulsions with the presence of asphaltene fractions. Therefore, the conversion rate of water was lower in the system with the presence of asphaltenes. On the other hand, for the asphaltene containing systems, the total gas consumption increased with a decrease of asphaltene polarity. This phenomenon could be attributed to the higher

conversion rate of water caused by the lower water droplet size for the emulsion with the less polar asphaltene fraction.

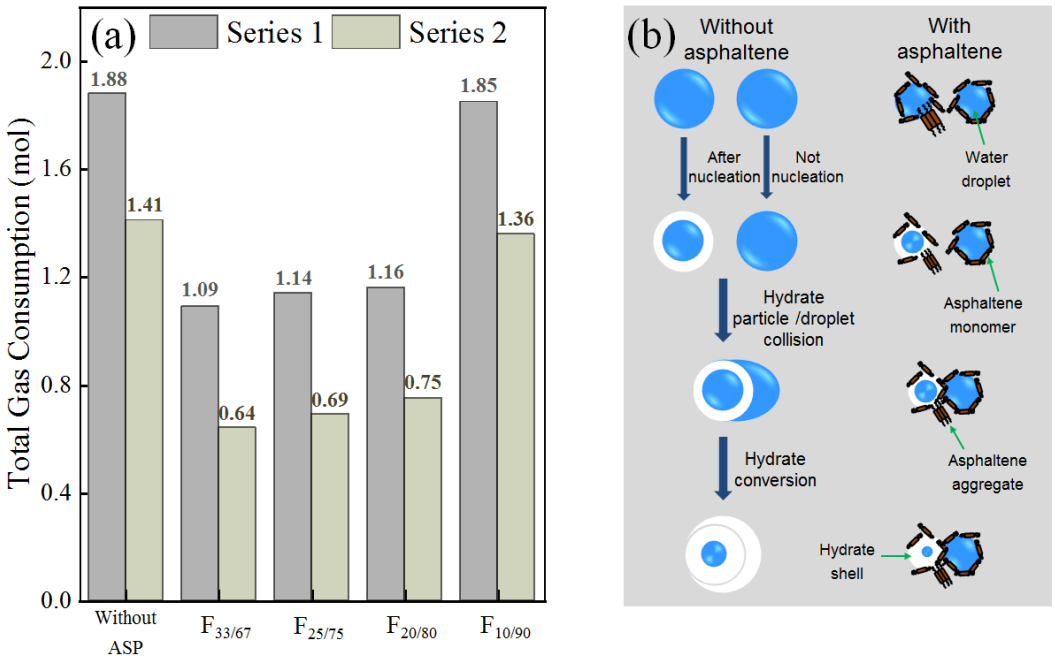

Figure 15. (a) Total gas consumtion for hydrate formation. (b) Schematic of the consequence of the collision of a droplet with a converting hydrate (modified from Turner[35]).

3.4 Influence of asphaltene polarity on hydrate dissociation

The dissociation percentages of the five hydrate systems for Series 1 experiments are shown in Figure 16. It was illustrated that the presence of asphaltenes can slightly promote hydrate dissociation. The dissociation percentage of fraction $F_{20/80}$ is ~10% higher than the system with the absence of asphaltenes. However, no linear relation between the dissociation rate and polarity of asphaltenes was found. For example, at 25 min, the dissociation percentage was 36.47%, 39.04%, 40.26%, 34.04%, and 31.99% in the system with fraction $F_{33/67}$, $F_{25/75}$, $F_{20/80}$, $F_{10/90}$ and without asphaltene fractions, respectively. This phenomenon could be attributed to the hydrate particle diameter and the amount of formed hydrates. In the systems with the same water cut, the lower hydrate particle diameter would enlarge the surface area of the hydrate and further increase the dissociation rate.[59-61]

The five hydrate systems can be divided into two groups according to the total gas consumption shown in Figure 15a. Group A consists of the three systems with fraction $F_{20/80}$, $F_{33/67}$, and $F_{25/75,}$ and group B includes two systems with fraction $F_{10/90}$ and without asphaltenes. As shown in Figure 16, the dissociation percentage of the three systems in group A is all higher than the systems in Group B. This was because that more heat was required for the dissociation of hydrate as a higher amount of formed hydrate in group B. On the other hand, in group A, the dissociation rate of the system with fraction $F_{20/80}$ is slightly higher than that with other fractions, and the same phenomenon was found of it with fraction $F_{10/90}$ in group B. This could be attributed to the higher surface area of hydrate particles caused by the lower size of hydrate particles. According to Kim et al.[59] and Goel et al.[60], the hydrate dissociation rate is proportional to the hydrate particle surface area. These data suggest that the hydrates are easier to be removed by heat stimulation in the system with asphaltenes, which can favor the operation and management of offshore oil and gas pipelines.

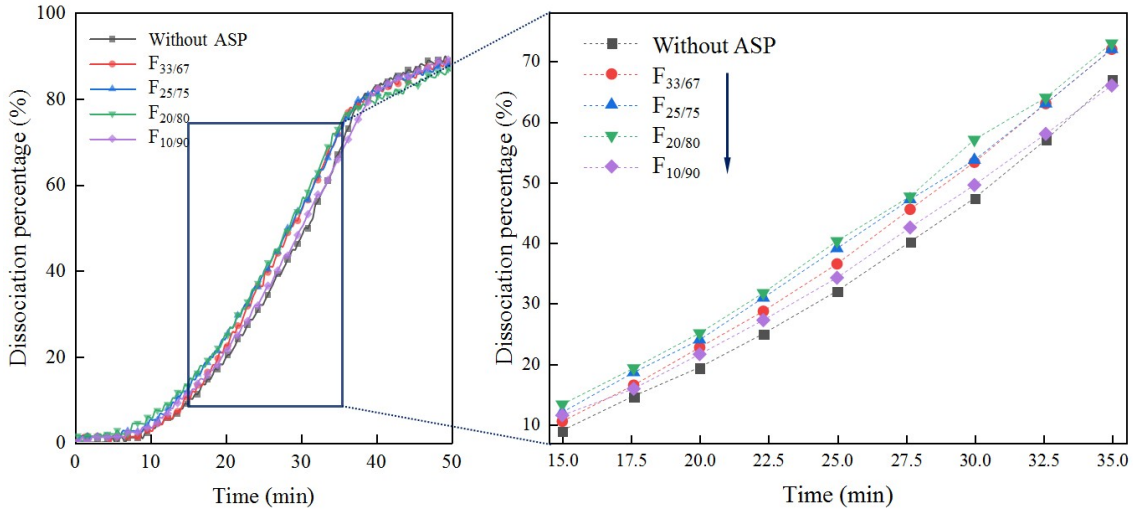

Figure 16. Dissociation percentage of hydrate formed in the emulsions with different polarity asphaltene fractions.

4. Conclusions

Asphaltenes were separated from a Venezuela residue oil and fractionated into four different polar fractions for investigating the influence of asphaltene polarity on hydrate nucleation,

growth and dissociation processes. It was observed that the particle size of asphaltene decreased with decreasing polarity. In addition, the more polar asphaltene fraction has a higher tendency of self-aggregation in emulsions due to the structural and compositional characteristics of a larger C/H ratio, higher aromaticity, and shorter length of alkyl side chain.

It was found that the presence of asphaltenes impeded hydrate nucleation, leading to a longer induction time. The adsorbed asphaltenes at the water-oil interface may be the primary mechanism of the inhibition effect. Moreover, the adsorption-inhibition effect on the nucleation of hydrate was more pronounced for the emulsion with the less polar asphaltene fraction. Therefore, the induction time increased with a reduction in asphaltene polarity. The amount of formed hydrate was found to decrease for the system with the presence of asphaltenes, which was more significant in the system with the presence of higher polarity asphaltene fraction. In addition, the fraction $F_{25/75}$, $F_{20/80}$, and $F_{10/90}$ all increased the growth rate of hydrate in the initial growth stage, which might be caused by the higher droplet surface area as the smaller water droplets, compared with the emulsion without asphaltenes. However, fraction $F_{33/67}$ significantly decreased the growth rate, which could be attributed to the restriction of mass transfer by the asphaltene aggregates. For the hydrate dissociation process, the four subfractions all presented the promoting effect, which may be attributed to the larger hydrate surface area. The influence of asphaltene polarity on hydrate particle aggregation and the synergistic effect between asphaltene and anti-agglomerants in the hydrate slurry system will be investigated in future work to have a realistic understanding of the asphaltene on hydrate risk management.

Acknowledgments

This work was financially supported by National Natural Science Foundation of China (NNSF, Grant No. 51534007).

References

[1] Sloan ED, Koh CA. Clathrate hydrates of natural gases. Boca Raton: CRC Press; 2007.

[2] Norris BWE, Zerpa LE, Koh CA, Johns ML, May EF, Aman ZM. Rapid assessments of hydrate blockage risk in oil-continuous flowlines. *J Nat Gas Sci Eng.* 2016;30:284-294.

[3] Sloan ED. Fundamental principles and applications of natural gas hydrates. *Nature.* 2003;426:353–363.

[4] Hammerschmidt EG. Formation of gas hydrates in natural gas transmission lines. *Ind Eng Chem.* 1934;26(8):851-855.

[5] Zheng S, Khrutphisit T, Fogler HS. Entrapment of water droplets in wax deposits from water-in-oil dispersion and its impact on deposit build-up. *Energy Fuels.* 2016;31(1):340-350.

[6] Chi Y, Sarica C, Daraboina N. Experimental investigation of two-phase gas-oil stratified flow wax deposition in pipeline. *Fuel.* 2019;247:113-125.

[7] Zhang D, Huang Q, Zheng H, Wang W, Cheng X, Li R, Li W. Effect of wax crystals on nucleation during gas hydrate formation. *Energy Fuels.* 2019;33(6):5081-5090.

[8] Turner DJ. Clathrate hydrate formation in water-in-oil dispersion. Golden, CO, USA: Colorado School of Mines. 2005.

[9] Aman ZM, Brown EP, Sloan ED, Sum AK, Koh CA. Interfacial mechanisms governing cyclopentane clathrate hydrate adhesion/cohesion. *Phys Chem Chem Phys.* 2011;13(44):19796-19806.

[10] Aman ZM, Dieker LE, Aspenes G, Sum AK, Sloan ED, Koh CA. Influence of model oil with surfactants and amphiphilic polymers on cyclopentane hydrate adhesion forces. *Energy Fuels.* 2010;24(10):5441-5445.

[11] Turner DJ, Miller KT, Dendy Sloan E. Methane hydrate formation and an inward growing shell model in water-in-oil dispersions. *Chem Eng Sci.* 2009;64(18):3996-4004.

[12] Shi B, Gong J, Sun C, Zhao J, Ding Y, Chen G. An inward and outward natural gas hydrates growth shell model considering intrinsic kinetics, mass and heat transfer. *Chem Eng J.* 2011;171(3):1308-1316.

[13] Dalmazzone D, Hamed N, Dalmazzone C. DSC measurements and modeling of the kinetics of methane hydrate formation in water-in-oil emulsion. *Chem Eng Sci.* 2009;64(9):2020-2026.

[14] Boxall J. Hydrate plug formation from <50% water content water-in-oil emulsions. Golden, CO, USA: Colorado School of Mines. 2009.

[15] Zerpa LE, Sloan ED, Sum AK, Koh CA. Overview of CSMHyK: A transient hydrate formation model. *J Petrol Sci Eng.* 2012;98-99:122-129.

[16] Daraboina N, Pachitsas S, von Solms N. Natural gas hydrate formation and inhibition in gas/crude oil/aqueous systems. *Fuel.* 2015;148:186-190.

[17] Gao S. Investigation of Interactions between gas hydrates and several other flow assurance elements. *Energy*

Fuels. 2008;22(5):3150-153.

[18] Chen Y, Shi B, Liu Y, Song S, Gong J. Experimental and theoretical investigation of the interaction between hydrate formation and wax precipitation in water-in-oil emulsions. *Energy Fuel.* 2018;32(9):9081-9092.

[19] Savvidis TG, Fenistein D, Barré L, Béhar E. Aggregated structure of flocculated asphaltenes. *AIChE J.* 2001;47(1):206-211.

[20] Zi M, Wu G, Li L, Chen D. Molecular dynamics simulations of methane hydrate formation in model water-in-oil emulsion containing asphaltenes. *J Phys Chem C.* 2018;122(41):23299-23306.

[21] Sztukowski DM, Jafari M, Alboudwarej H, Yarranton HW. Asphaltene self-association and water-in-hydrocarbon emulsions. *J Colloid Interf Sci.* 2003;265(1):179-186.

[22] Sandoval GAB, Thompson RL, Sad CMS, Teixeira A, Soares EJ. Influence of adding asphaltenes and gas condensate on CO_2 hydrate formation in water-CO_2-oil systems. *Energy Fuels.* 2019;33(8):7138-7146.

[23] Stoporev AS, Manakov AY, Altunina LK, Strelets LA, Kosyakov VI. Nucleation rates of methane hydrate from water in oil emulsions. *Can J Chem.* 2015;93(8):882-887.

[24] Nalwaya V, Tantayakom V, Piumsomboon P, Fogler S. Studies on Asphaltenes through analysis of polar fractions. *Ind Eng Chem Res.* 1999;38(3):964-972.

[25] Wattana P, Fogler HS, Yen A, Carmen Garcìa MD, Carbognani L. Characterization of polarity-based asphaltene subfractions. *Energy Fuels.* 2005;19(1):101-110.

[26] Li C, Zhu H, Yang F, Liu H, Wang F, Sun G, Yao B. Effect of asphaltene polarity on wax precipitation and deposition characteristics of waxy oils. *Energy Fuels.* 2019;33(8):7225-7233.

[27] Zhang L, Yang G, Wang J, Li Y, Li L, Yang C. Study on the polarity, solubility, and stacking characteristics of asphaltenes. *Fuel.* 2014;128:366-372.

[28] Lobato MD, Gámez F, Lago S, Pedrosa JM. The influence of the polarity of fractionated asphaltenes on their Langmuir-film properties. *Fuel.* 2017;200:162-170.

[29] Li Y, Han S, Lu Y, Zhang J. Influence of asphaltene polarity on crystallization and gelation of waxy oils. *Energy Fuels.* 2018;32(2):1491-1497.

[30] Xue H, Zhang J, Han S, Sun M, Yan X, Li H. Effect of asphaltenes on the structure and surface properties of wax crystals in waxy oils. *Energy Fuels.* 2019;33(10):9570-9584.

[31] Li H, Zhang J, Xu Q, Hou C, Sun Y, Zhuang Y, Han S, Wu C. Influence of asphaltene on wax deposition: Deposition inhibition and sloughing. *Fuel.* 2020;266:117047.

[32] Wang W, Huang Q, Zheng H, Wang Q, Zhang D, Cheng X, Li R. Effect of wax on hydrate formation in water-in-oil emulsions. *J Disper Sci Technol.* 2019:1-10.

[33] Zheng H, Huang Q, Wang W, Long Z, Kusalik PG. Induction time of hydrate formation in water-in-oil emulsions. *Ind Eng Chem Res.* 2017;56(29):8330-8339.

[34] Song S, Shi B, Yu W, Ding L, Chen Y, Yu Y, Ruan C, Liu Y, Wang W, Gong J. A new methane hydrate decomposition model considering intrinsic kinetics and mass transfer. *Chem Eng J.* 2019;361:1264-1284.

[35] Turner DJ, Miller KT, Sloan ED. Direct conversion of water droplets to methane hydrate in crude oil. *Chem Eng Sci.* 2009;64(23):5066-5072.

[36] Liu Z, Vasheghani Farahani M, Yang M, Li X, Zhao J, Song Y, Yang J. Hydrate slurry flow characteristics influenced by formation, agglomeration and deposition in a fully visual flow loop. *Fuel*. 2020;277:118066.

[37] Lv X, Zuo J, Liu Y, Zhou S, Lu D, Yan K, Shi B, Zhao H. Experimental study of growth kinetics of CO_2 hydrates and multiphase flow properties of slurries in high pressure flow systems. *Rsc Adv*. 2019;9:32873-32888.

[38] Zhou S, Yan H, Su D, Navaneethakannan S, Chi Y. Investigation on the kinetics of carbon dioxide hydrate formation using flow loop testing. *J Nat Gas Sci Eng.* 2018;49:385-392.

[39] Liu Y, Shi B, Ding L, Ma Q, Chen Y, Song S, Zhang Y, Yong Y, Lv X, Wu H, Wang W, Gong J. Study of hydrate formation in water-in-waxy oil emulsions considering heat transfer and mass transfer. *Fuel.* 2019;244:282-295.

[40] Liu D, Li C, Zhang X, Yang F, Sun G, Yao B, Zhang H. Polarity effects of asphaltene subfractions on the stability and interfacial properties of water-in-model oil emulsions. *Fuel.* 2020;269:117450.

[41] Rogel E, León O, Torres G, Espidel J. Aggregation of asphaltenes in organic solvents using surface tension measurements. *Fuel.* 2000;79(11):1389-1394.

[42] Gao P, Zhang J, Ma G. Direct image-based fractal characterization of morphologies and structures of wax crystals in waxy crude oils. Journal of Physics: *Condensed Matter.* 2006;18(50):11487-51106.

[43] Ma C, Lu Y, Chen C, Feng K, Li Z, Wang X, Zhang J. Electrical treatment of waxy crude oil to improve its cold flowability. *Ind Eng Chem Res.* 2017;56(38):10920-10928.

[44] McLean JD, Kilpatrick PK. Effects of asphaltene aggregation in model heptane-toluene mixtures on stability of water-in-oil emulsions. *J Colloid Interf Sci.* 1997;196(1):23-34.

[45] Czarnecki J, Tchoukov P, Dabros T, Xu Z. Role of asphaltenes in stabilisation of water in crude oil emulsions. *Can J Chem Eng.* 2013;91(8):1365-1371.

[46] Dabros T, Yeung A, Masliyah J, Czarnecki J. Emulsification through area contraction. *J Colloid Interface Sci.* 1999;210(1):222-224.

[47] Simon S, Sjöblom J, Wei D. Interfacial and emulsion stabilizing properties of indigenous acidic and esterified asphaltenes. *J Disper Sci Technol.* 2016;37(12):1751-1759.

[48] Sloan ED, Fleyfel F. A molecular mechanism for gas hydrate nucleation from ice. *AIChE J.* 1991;37(9):1281-1292.

[49] Takeya S, Hori A, Hondoh T, Uchida T. Freezing-memory effect of water on nucleation of CO_2 hydrate crystals. *J Phys Chem B.* 2000;104(17):4164-4168.

[50] Lv Y, Sun C, Liu B, Chen G, Gong J. A water droplet size distribution dependent modeling of hydrate formation in water/oil emulsion. *AIChE J.* 2017;63(3):1010-1023.

[51] Soave G. Equilibrium constants from a modified Redlich-Kwong equation of state. *Chem Eng Sci.* 1972;27(6):1197-1203.

[52] Li S, Sun C, Liu B, Feng X, Li F, Chen L, Chen G. Initial thickness measurements and insights into crystal growth of methane hydrate film. *AIChE J.* 2013;59(6):2145-2154.

[53] Taylor CJ, Miller KT, Koh CA, Sloan ED. Macroscopic investigation of hydrate film growth at the hydrocarbon/water interface. *Chem Eng Sci.* 2007;62(23):6524-6533.

[54] Li B, Liu G, Xing X, Chen L, Lu X, Teng H, Wang J. Molecular dynamics simulation of CO_2 dissolution in heavy oil resin-asphaltene. *J CO_2 Util.* 2019;33:303-310.

[55] Dmitrievskii AN, Pribylov AA, Skibitskaya NA, Zekel LA, Kubyshkin AP, Shpirt MY. Sorption of butane, propane, ethane, methane, and carbon dioxide on asphaltene. *Russ J Phys Chem.* 2006;80(7):1099-1104.

[56] Sharifi H, Englezos P. Accelerated hydrate crystal growth in the presence of low dosage additives known as kinetic hydrate inhibitors. *J Chem Eng Data.* 2014;60(2):336-342.

[57] Cha M, Shin K, Seo Y, Shin J, Kang S. Catastrophic growth of gas hydrates in the presence of kinetic hydrate inhibitors. *J Phys Chem A.* 2013;117(51):13988-13995.

[58] Sharifi H, Ripmeester J, Walker VK, Englezos P. Kinetic inhibition of natural gas hydrates in saline solutions and heptane. *Fuel.* 2014;117:109-117.

[59] Kim HC, Bishnoi PR, Heidemann RA, Rizvi SSH. Kinetics of methane hydrate decomposition. *Chem Eng Sci.* 1987;42(7):1645-1653.

[60] Goel N, Wiggins M, Shah S. Analytical modeling of gas recovery from in situ hydrates dissociation. *J Petrol Sci Eng.* 2001;29(2):115-127.

[61] Clarke M, Bishnoi PR. Determination of the intrinsic rate of ethane gas hydrate decomposition. *Chem Eng Sci.* 2000;55(21):4869-4883.